ELSEVIER

Biophysical Chemistry 125 (2007) 403–410

Biophysical Chemistry

http://www.elsevier.com/locate/biophyschem

Property of the M-DNA probed by a minor groove binding dye 4′,6-diamidino-2-phenylindole

Jong-Sub Shin [a], Jong-Moon Kim [a], Hyun Mee Lee [a], Jae-Hyung Kim [b], Hyosun Lee [c], Seog K. Kim [a,*]

[a] Department of Chemistry, Yeungnam University, Gyeongsan City, Gyeong-buk, 712–749, Republic of Korea
[b] Dong-il Shimadzu Biotech. #393-4, Doryong-dong, Yuseong-ku, Daejeon, 305–340, Republic of Korea
[c] Department of Chemistry, Kyungpook National University, 1370 Sankyuk-dong, Buk-gu, Daegu, 702–701, Republic of Korea

Received 29 August 2006; received in revised form 4 October 2006; accepted 6 October 2006
Available online 11 October 2006

Abstract

Spectral properties including circular and linear dichroism (CD and LD) of M-DNA, a molecular electric wire, formed at a high Zn^{2+} concentration have been studied using a minor groove binding drug 4′,6-diamidino-2-phenylindole (DAPI) as a probe. As the Zn^{2+} concentration increased, the magnitude of LD in the DNA absorption region decreased at pH 8.5, implying the aggregation of DNA, which is in contrast with the retained LD magnitude at pH 7.0. As the M-DNA formed, change in the secondary structure of DNA was observed by CD spectrum, which resembles that of the C-form DNA, although overall structure seemed to remain as a right handed double helix. The DAPI–DNA complex in the presence of high concentration of Zn^{2+} ions at pH 7.0 exhibited the similar CD spectrum with that in the absence of Zn^{2+} ion, consisting of type I, II and III. In contrast, at pH 8.5 at a high Zn^{2+} concentration in which DNA is in its M-form, DNA bound DAPI produced only the type III CD, suggesting that DAPI binds at the surface of M-DNA: the presence of Zn^{2+} ions prevents the minor groove binding of DAPI.

Keywords: DNA; M-DNA; Minor groove; 4′,6-Diamidino-2-phenylindole; Polarized spectroscopy; Binding mode

1. Introduction

In recent years, M-DNA, a complex formed between divalent metal ions and DNA, which acts as a molecular wire, has been drawing attention for its electrical properties and for its potential applications to nanotechnology [1]. One of the recent applications, detection of single-nucleotide mismatches using M-DNA, was reported [2] which highlighted the importance of understanding the properties of M-DNA. Its electric conducting property of M-DNA has been also reported [1,3–5]. In the presence of Zn^{2+}, Co^{2+} or Ni^{2+} at pH 8.5, electron transfer occurred from fluorescein donor to rhodamine acceptor through up to 54 base pairs long double stranded oligonucleotide [4]. Direct measurement of the current as a function of voltage on M-DNA formed from λ DNA showed a linear relationship between current and applied voltage, providing evidence for conduction through M-DNA [5]. Upon adding divalent cations, intercalated ethidium was extruded at a pH above 8.0 [6], which has been regarded as an indication for the formation of M-DNA. A recent atomic force microscopy study showed that the DNA modified with nickel or cobalt cations suffered condensation in which length reduced fivefold and the height increased by nearly one order of magnitude [7]. Two sets of base-pairing schemes, one in which the amino protons of thymine and guanine base are replaced by the metal ion or, alternatively, an amino proton of adenine and cytosine base is removed, have been proposed for M-DNA (Fig. 1) [4,5]. The latter base-pair requires the enol tautomers of thymine and guanine. The metal ions located in the minor groove in the former two base-pairs and in the major groove in the latter case.

4′,6-Diamidino-2-phenylindole (DAPI, Fig. 1) has been well known to bind at the minor groove of DNA preferably at 4–6 contiguous AT base pairs [8–15]. Upon binding to DNA, DAPI exhibited three distinguishable induced CD spectra in the DAPI absorption region, depending mainly on the [drug]/[DNA] ratio

* Corresponding author. Tel.: +82 53 810 2362; fax: +82 53 815 5412.
E-mail address: seogkim@yu.ac.kr (S.K. Kim).

0301-4622/$ - see front matter © 2006 Published by Elsevier B.V.
doi:10.1016/j.bpc.2006.10.002

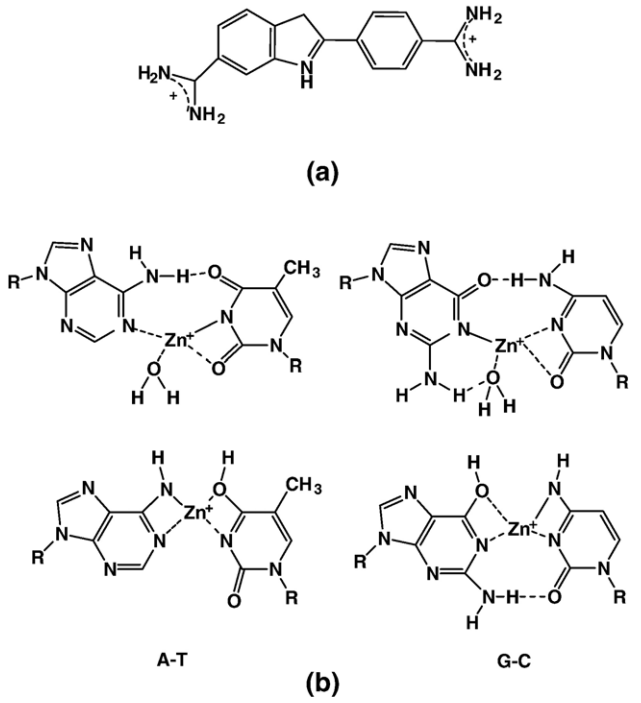

Fig. 1. Molecular structure of (a) 4′,6-diamidino-2-phenylindole and (b) proposed minor and major groove chelating sites of Zn^{2+} ion. Zn^{2+} binds at the major groove in the bottom two diagrams.

(R ratio) [8–11]. A positive CD with its maximum at 335 nm at low R ratio (Type I), and a new positive CD at 375 nm at an intermediate R ratios were apparent (Type II). Further increasing in the R ratios above 0.15, a very small negative CD feature above 400 nm and the decrease in the type II CD were apparent (Type III). X-ray structure and NMR studies revealed that DAPI indeed locates in the minor groove of oligonucleotides and is stabilized by formation of hydrogen bonds and hydrophobic effects [12–15]. In this work, spectroscopic properties of DAPI bound to DNA in the presence of Zn^{2+} ions at pH = 8.5 were compared with those at pH 7.0. It was assumed that the spectroscopic properties of DAPI bound to M-DNA are expected to be altered to a great extent if metal ions are bound at the minor groove while the effect of metal ions would be little if metal ions are bound at the major groove.

2. Materials and methods

2.1. Materials

All chemicals were purchased from Sigma and were used without further purification except for calf thymus DNA (referred to as DNA). DNA was dissolved in pH 7.0, 5 mM cacodylate buffer containing 1 mM EDTA and 100 mM NaCl by exhaustive stirring at 4 °C. Dissolved DNA was dialyzed several times at 4 °C in 10 mM Tris buffer containing 10 mM NaCl at pH 7.0 and pH 8.5. Desired Zn^{2+} concentration was achieved by adding $Zn(ClO_4)_2$ and the same concentration of $NaClO_4$ because the addition of $ZnCl_2$ resulted in a DNA aggregation at relatively low Zn^{2+} concentrations. The concentrations of DNA, ethidium and DAPI were measured spectrophotometrically using the extinction coefficients: $\varepsilon_{343\ nm} = 27{,}000\ M^{-1}\ cm^{-1}$ for DAPI, $\varepsilon_{480\ nm} = 5800\ M^{-1}\ cm^{-1}$ for ethidium, and $\varepsilon_{258\ nm} = 6700\ M^{-1}\ cm^{-1}$ for DNA.

2.2. Polarized spectroscopy

A CD spectrum is induced for DNA in the bases absorption region due to chiral arrangement of the base transitions, which provide the information for the secondary structure of DNA. DAPI does not contain any chiral center either but acquires a strong CD in the DAPI's lowest absorption region (300 nm–350 nm) when bound to DNA. The origin of the induced CD signal is believed to be the nondegenerated coupling between the electric transition moment of DAPI and those of the chirally arranged DNA base (pairs) [16]. Three types of the induced CD for DAPI that associated with double stranded DNA have been noticed [8]. CD spectrum of the DAPI–DNA complex was recorded on a Jasco J715 spectropolarimeter using a 1-cm quartz cell.

Linear dichroism (LD) is the difference in absorbance between the light plane polarized parallel and perpendicular to the flow direction [17–19]. Measured LD spectrum is divided by an isotropic absorption spectrum to give dimensionless quantity reduced LD, LD^r, which is related to the orientation and optical factor as

$$LD^r = 3S\left(\frac{<3\cos^2\alpha> - 1}{2}\right) \quad (1)$$

The orientation factor, S, reflects the degree of DNA orientation which depends on the contour length and flexibility of DNA, viscosity and temperature of the medium. The value of S is between 0 and 1 such that $S = 0$ for random orientation and is 1 for perfectly oriented sample. The symbol α denotes the angle between the local DNA helix axis (flow direction) and the electric transition moment of DNA bound drugs. It is determined from the DNA base dichroism at 260 nm, assuming an effective angle of 86° between the $\pi^* \leftarrow \pi$ transition of the nucleo-bases and the DNA helix axis [20,21]. LD spectra were recorded on a Jasco J810 spectropolarimeter equipped with a flow-orienting Couette cell device with an inner rotating cylinder [22]. Polarized light spectra were averaged over an appropriate number of scans when it is necessary.

2.3. Fluorescence measurements

Fluorescence intensity of the ethidium–DNA complex decreases upon formation of M-DNA because ethidium does not intercalate to M-DNA. Hence, the formation of M-DNA can be conveniently monitored by an ethidium fluorescence assay [1,6]. The intensity of ethidium was measured at 480 nm excitation and 535 nm emission. Slit widths were 5 nm for both excitation and emission. On the other hand, fluorescence intensity of DAPI, which is enhanced by binding at the minor groove of DNA due to stripping off the surrounding water molecules and the change in the molecular conformation [8,10],

was not decreased even at pH 8.5. I_2 has been occasionally used as a fluorescence quencher for probing the binding mode of DAPI to various DNAs [23–25]. If the fluorescence quenching occurs through a simple static or a dynamic mechanism, the ratio of the fluorescence intensity in the presence (F) to the absence (F_0) of quencher is expected to be a straight line in the Stern–Volmer plot [26].

$$\frac{F_0}{F} = 1 + K_{SV}[Q] \quad (2)$$

Where K_{SV} represents either the static or dynamic quenching constant, and denotes the concentration of the quencher. In the DAPI–DNA complex case, the fluorescence quenching by I_2 appeared to be an upward bending curve in the Stern–Volmer plot (see Results section). Such positive deviations may be interpreted in terms of a "sphere of action", which is described by a modified Stern–Volmer equation.

$$\frac{F_0}{F} = (1 + K_D[Q])\exp([Q]VN/1000) \quad (3)$$

Where K_D represents the dynamic quenching constant. V is the volume of the sphere, in which closely spaced fluorophore-quencher pairs are immediately quenched and thus the probability of the static quenching is unity. The dynamic quenching efficiency, K_D, may be determined independently by measuring the fluorescence decay time in the absence and presence of the quencher similarly with Eq. (2).

$$\frac{\langle\tau_0\rangle}{\langle\tau\rangle} = 1 + k_q\langle\tau_0\rangle[Q] = 1 + K_D[Q] \quad (4)$$

Where k_q is the bimolecular quenching constant. The average decay time for the multi-decay process in the absence and presence of quencher, $\langle\tau_0\rangle$ and $\langle\tau\rangle$ is defined by $\langle\tau\rangle = \sum_i a_i\tau_i^2 / \sum_i a_i\tau_i$ [27].

The fluorescence intensities of the DAPI–DNA complex in the presence and absence of I_2 were monitored on a Jasco FP-777 spectroflurometer at 360 nm excitation and 460 nm emission. Slit widths for both excitation and emission were 5 nm. The fluorescence intensities were recorded using an IBH 5000U fluorescence life time system. The LED source of a nanoLED-3, which produces an excitation radiation at 370 nm with fwhm of ~ 1.3 ns, was used to excite the DAPI–DNA complex and the emission was detected at 460 nm with slit width 16 nm and 16 nm for excitation and emission, respectively.

3. Results

3.1. Polarized light spectra of M-DNA

A molecular wire, M-DNA, is a complex formed between divalent metal ions and duplex DNA at high pH. The CD spectra of DNA at pH 7.0 and 8.5 in the presence of various concentrations of Zn^{2+} ions are depicted in Fig. 2. In the absence of Zn^{2+} ion, DNA exhibited an ordinary B-form in the CD spectrum at both pH 7.0 and 8.5 (in comparison to solid curve spectrum both in panel (a) and (b)). DNA seems to remain as the B form (Fig. 2(a)) at pH 7.0 even at a high Zn^{2+} concentration although some decrease in the CD intensity at the positive CD band (~ 280 nm) was observed. In contrast, large changes in CD spectrum were observed at pH 8.5 with increasing Zn^{2+} concentration (Fig. 2(b)). At $[Zn^{2+}]$ = 150 μM, the positive band at long wavelength split into two positive bands at ~ 265 nm and ~ 288 nm while the negative band at short wavelength remained. The A-form DNA is reminiscent of part of this CD spectrum with respect to the positive band developing near 265 nm. However, this CD spectrum may not represent M-DNA because intercalated ethidium remained to be intercalated (see below). As the Zn^{2+} concentrations increased further, the positive CD maximum at ~ 265 nm disappeared, while the band at long wavelength retained. The shape of the CD spectrum at $[Zn^{2+}]$ = 600 μM is similar to that observed from the C-DNA [34,35]. This Zn^{2+} concentration dependent change in the CD spectrum at pH 8.5 indicates that the conformation change from B- to M-DNA by Zn^{2+} ion is not a simple two-phase transformation.

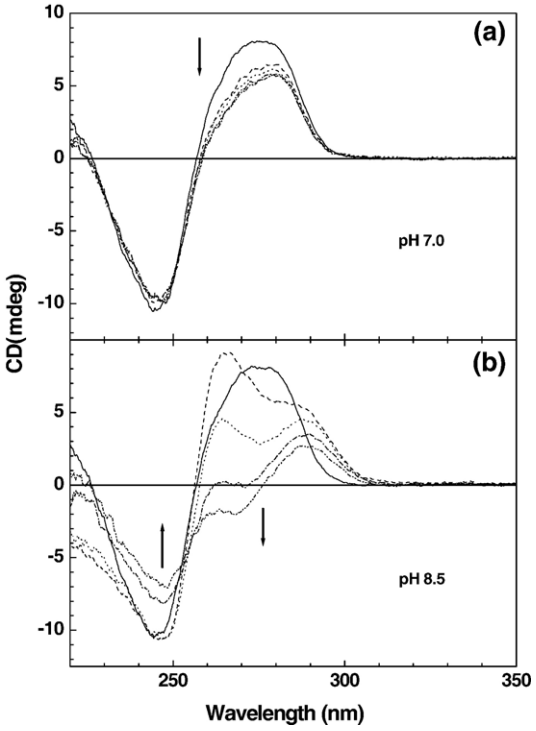

Fig. 2. CD spectrum of DNA at pH 7.0 (panel a) and 8.5 (panel b) in the presence of various concentrations of Zn^{2+} and its absence. In the direction of arrow, $[Zn^{2+}]$ = 0, 150, 300, 450, 600 μM. [DNA] = 100 μM.

The magnitude of LD depends on the contour length and the flexibility of the DNA as long as the viscosity and the temperature of the solution do not change [16–18]. Zn^{2+} concentration dependent LD spectrum of DNA at pH 7.0 and 8.5 are depicted in Fig. 3(a). The LD spectra at all conditions exhibit negative values with its shape resembles with DNA absorption spectrum which was expected from the experimental set-up employed in this work [12]. The magnitude of LD at pH 8.5 (curve a) is somewhat larger compared to that at pH 7.0 (curve b) in the absence of Zn^{2+} ion, which may be attributed to

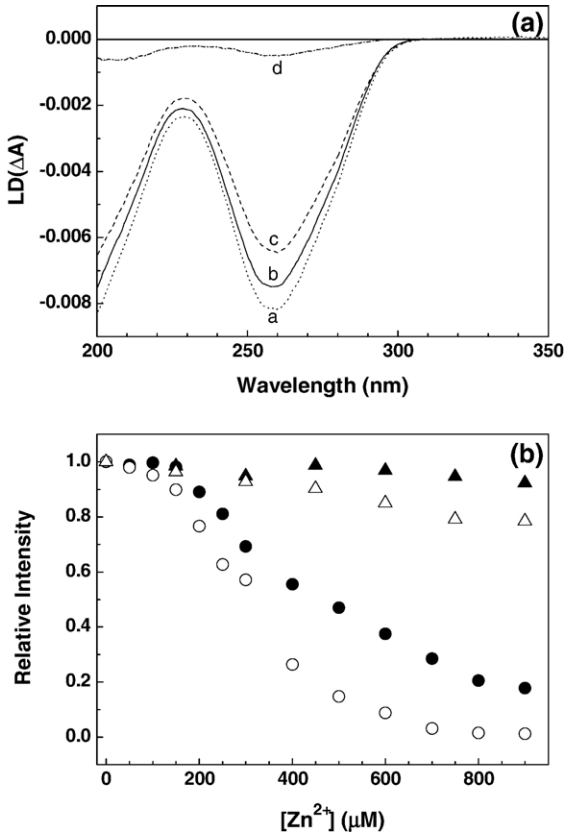

Fig. 3. (a) LD spectrum of DNA at pH 7.0 and 8.5 in the presence and absence of 600 μM Zn^{2+}. Curve a: pH 8.5, [Zn^{2+}]=0 μM, curve b: pH 7.0, [Zn^{2+}]=0 μM, curve c: pH 7.0, [Zn^{2+}]=600 μM, curve d: pH 8.5, [Zn^{2+}]=600 μM. [DNA]=100 μM. (b) Change in the LD magnitude of DNA at 260 nm with respect to [Zn^{2+}] concentration at pH 7.0 (opened triangle) and at pH 8.5 (opened circle) and changes in the fluorescence intensity of the ethidium–DNA complex at pH 7.0 (closed triangle) and pH 8.5 (closed circle). The ethidium–DNA complex was excited at 535 nm and emission was detected at 590 nm for fluorescence measurement. Slit widths=5 nm for both excitation and emission. [DNA]=100 μM and [ethidium]=5 μM.

the smaller amount of positive ions at low pH. Positive ions are believed to bind at the phosphate groups of DNA by electrostatic interactions, decreasing the repulsive interaction between the negatively charged phosphate groups thereby, resulting in the increased flexibility of DNA. The presence of 700 μM Zn^{2+} ions result in an approximately 15% decrease in the LD magnitude (Fig. 3(b)) at pH 7.0. On the other hand, at pH 8.5, the magnitude of LD decreased to a small extent at the Zn^{2+} concentrations below 150 μM then a large decrease followed as the Zn^{2+} concentration further increased. LD magnitude reached zero at [Zn^{2+}]=700 μM at pH 8.5, indicating that M-DNA does not orient in the flow. It is also indicative that change in CD spectrum of DNA below ~ 150 μM Zn^{2+} is not related to the formation of M-DNA. As mentioned before, formation of M-DNA can be followed by the extrusion of intercalated ethidium which is accompanied by a decrease in the fluorescence intensity. At pH 8.5, gradual decrease in the fluorescence intensity of ethidium with increasing Zn^{2+} concentration, which reflects the formation of M-DNA, is comparable with decrease in the LD magnitude. As it was observed from the LD spectrum, and in agreement with the other report [6], the fluorescence intensity did not change below [Zn^{2+}] ≈ 150 μM, at which Zn^{2+} was suggested to bind to the phosphate groups of DNA. On the other hand, a very small decrease in the fluorescence intensity was observed at pH 7.0 up to [Zn^{2+}]=900 μM.

3.2. Absorption and CD of M-DNA bound DAPI

The absorption spectrum of DAPI bound to DNA at pH 7.0 and 8.5 in the presence of 600 μM Zn^{2+} is compared in Fig. 4(a) and (b). At both pHs, an increase in the [DAPI]/[DNA] ratio (R ratio) resulted in some blue-shift in the absorption spectrum: absorption maximum at 361 nm shifted to 353 nm at pH 7.0 while 355 nm shifted to 350 nm at pH 8.5. Absorbance at the low pH was unchanged but decreased at the high pH. A small hypochromism was also apparent at high pH. An isosbestic point observed at 391 nm and 397 nm, respectively, at pH 7.0 and 8.5 indicates the R ratio dependent binding mode of DAPI to both B- and M-DNA is composed of at least two species. The induced CD spectrum of DAPI bound to B-DNA at pH 7.0 in the presence of 600 μM Zn^{2+} showed similar pattern with that measured in the absence of metal ion (Fig. 5(a)). At a very low R ratio, the CD spectrum is characterized by a single positive peak with its maximum at ~ 335 nm (type I). As the R ratio increased to 0.12, so called type II CD spectrum which was attributed to DAPI binds at the minor groove of DNA whose conformation changed by the binding of the first DAPI, consist of a positive band with its maximum at 365 nm. At the intermediate mixing ratios, the appearance of the CD spectrum can be described by the combination of Type I and II CD spectrum with an isodichroic point at 349 nm. The intensity of type II CD decreased with further increase in the R ratio. In contrast with pH 7.0, CD spectrum of the DAPI–M-DNA complex did not exhibit any type I CD at pH 8.5 (Fig. 5(b)). Even at a very low R ratio, the shape of the CD spectrum appeared to be of type II. The addition of more DAPI (increasing the R ratio) resulted in a

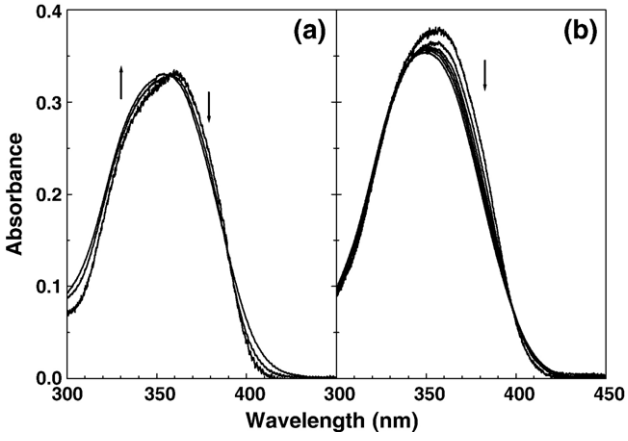

Fig. 4. Mixing ratio dependent absorption spectrum of DAPI in the presence of DNA and Zn^{2+} at pH 7.0 (panel a) and 8.5 (panel b). At pH 7.0, [DAPI]=2, 6, and 12 μM and at pH=8.5. [DAPI]=2, 4, 6, 8, 10, and 12 μM. [DNA]=100 μM. The concentration of DAPI increases in the direction of the arrow. The spectra were normalized to the highest DAPI concentration for ease of comparison.

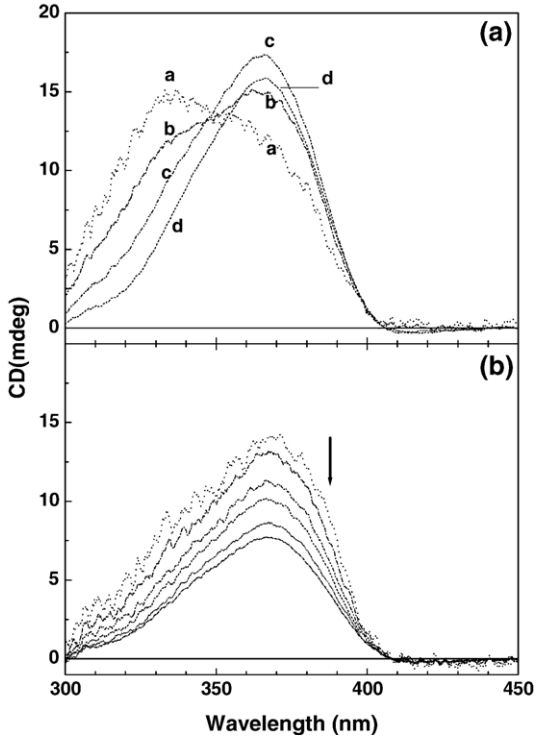

Fig. 5. Mixing ratio dependent induced CD spectrum of DAPI in the presence of 100 μM DNA and 600 μM Zn^{2+} at pH 7.0 (panel a) and 8.5 (panel b). In panel (a) (at pH 7.0), the DAPI concentrations were 2, 6, 12 and 20 μM which are denoted by curves a, b, c and d, respectively. At pH=8.5 (in panel (b)), [DAPI]=2, 4, 6, 8, 10, and 12 μM. The concentration of DAPI increases in the direction of the arrow. The spectra were normalized to the highest DAPI concentration for easy of comparison.

decrease in the CD intensity. However, a decrease in the CD intensity may not attribute to the release of the DAPI molecule from M-DNA because the absorption spectrum at the corresponding R ratio is different from that of the mixture of M-DNA-free and -bound DAPI.

3.3. Fluorescence quenching

A Stern–Volmer plot for quenching of the DNA bound DAPI by I_2 at pH 7.0 and 8.5 in the presence of 600 μM Zn^{2+} is depicted in Fig. 6. At pH 7.0, despite the presence of Zn^{2+} ion, I_2 quencher is inaccessible to DAPI which is the same as in the absence of Zn^{2+} [23–25]. At a high pH, an upward bending curve was observed. This type of curves may be understood by the sphere of action model [26]. Fluorescence decay time of DNA-free DAPI and DAPI bound to various DNA have been reported [28–32]. One, two and three decay times for DAPI–DNA complex have been reported depending on the conditions and set-ups. However, two decay component analysis may be the most rational because neither χ^2 value nor residuals were significantly improved by three component analysis. Fluorescence decay times of DAPI in the presence of Zn^{2+} ion were 0.10 ~ 0.15 ns and ~ 3.6 ns at pH 8.5 while the short component becomes a little longer at pH 7.0 (~ 0.26 ns) in the similar range with reported values. In the presence of various concentrations of I_2, the average fluorescence decay time remains, indicating that the dynamic quenching effect by I_2 on M-DNA bound DAPI is negligible. Then, from Eq. (3), the resulting modified Stern–Volmer plot should be an exponential curve. However, the result presented in Fig. 6 did not fit in any single exponential curve, indicating that the nature of the fluorescence quenching of the M-DNA bound DAPI by I_2 can not be described by a simple inner sphere mechanism. However, it is conclusive that DAPI bound to M-DNA is exposed more than that bound to B-DNA. Although detailed analysis of the quenching mechanism may be interesting, it is not in the scope of this work.

3.4. Dependence of LD^r spectrum of DAPI–DNA complex on the Zn^{2+} concentration

LD^r spectra of the DAPI–DNA complex, obtained by dividing measured LD by isotropic absorption spectrum, at pH 7.0 and 8.5 in the presence of various concentrations of Zn^{2+} are depicted in Fig. 7(a) and (b), respectively. In the absence of the metal ions, the shape of the LD^r spectra are similar at both pHs, characterized by a negative band at DNA absorption region (200 nm–300 nm) and a wavelength-dependent positive signal at DAPI absorption region (300 nm–400 nm). As the Zn^{2+} concentration increased to 300 μM, the positive LD^r signal above 300 nm became constant (wavelength-independent) while that at 150 μM exhibited an intermediate LD^r signal at pH 7.0. The concentration below 200 μM, Zn^{2+} was suggested to bind at the surface of DNA [5,6]. In contrast, the overall magnitude of LD^r signal decreased with increasing Zn^{2+} concentration at pH 8.5, suggesting that at least part of DNA was aggregated (see Discussion). The shape of the LD^r was similar to that measured at pH 7.0 although the magnitude is smaller, which suggests that the LD^r signal observed at high Zn^{2+} concentrations may be originated from the similar DAPI conformation. Similarly in the absence of DAPI, the LD^r magnitude is larger at pH 8.5 compared to that at pH 7.0 in the absence of Zn^{2+}, indicating that the DNA orients better at higher pH.

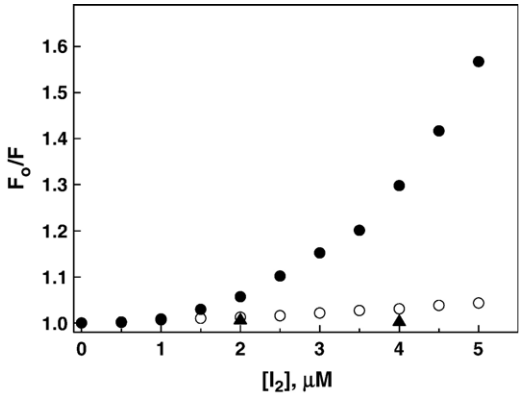

Fig. 6. The ratio of the fluorescence intensity of the DAPI–DNA complex in the absence of I_2 to its presence (Stern–Volmer plot) in the presence of 600 μM Zn^{2+}. The sample was excited at 360 nm and fluorescence was detected at 460 nm. Silt widths: 3/3 nm for both excitation and emission. Closed circles: pH 8.5, opened circle: pH 7.0. The ratio of the fluorescence decay time at pH 8.5 is shown (triangles). [DNA]=100 μM, [DAPI]=2 μM.

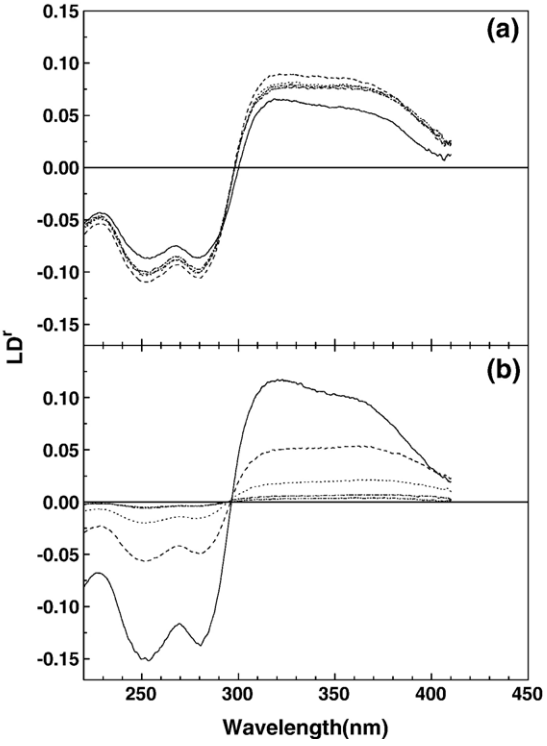

Fig. 7. LD^r spectrum of the DAPI–DNA complex at pH 7.0 (panel a) and pH 8.5 (panel b) at various Zn^{2+} concentrations obtained by dividing the measured LD by isotropic absorption spectrum. [DNA]=100 μM, [DAPI]=12 μM. [Zn^{2+}] are 0, 150, 300, 450, and 600 μM.

Two electric transition moments of DAPI have been reported at this absorption region [33]: the transition moment giving rise to absorption at 380 nm is polarized parallel to the indole-phenyl bond and that at 340 nm polarized at +15° (or −15°). The angle, α, which is the angle of the DAPI transition moment with respect to the local DNA helix axis, calculated from LD^r spectrum was ~ 40.0° at 340 nm and 42.8° at 380 nm at pH 7.0 in the absence of Zn^{2+} ions. The angle of 40°–45° is typical for the minor groove binding drugs [17–19]. In the presence of 150 μM Zn^{2+}, a small variation in the angle was observed to be 38.3° and 40.1°, respectively at 340 and 380 nm. In the absence of Zn^{2+} ion, these angles are nearly identical at pH 8.5 (39.0° and 40.1°). However, the presence of Zn^{2+} ions resulted in a smaller angle of ~ 35° at pH 8.5. A positive contribution around 270 nm is also apparent which may be the positive contribution of DAPI's electric transition or may reflect the distortion of the DNA base upon DAPI binding. However, the origin of this positive LD^r signal is uncertain therefore, is not analyzed in this work.

4. Discussion

4.1. Effect of Zn^{2+} on DNA conformation

Increasing the Zn^{2+} concentration to B form DNA (at pH 7.0) resulted in a small decrease in the positive band in the long wavelength region and a decrease in the LD magnitude. In the LD case, the shape of the spectrum remains. Intercalated ethidium remains to be intercalated. All these observations indicate that the change in the secondary structure of DNA is minimal. At pH 8.5 at relatively low concentrations, and at pH 7.0, Zn^{2+} ions have been suggested to interact with the phosphate groups of DNA [6]. In contrast, changes in the spectral properties of DNA are drastic at pH 8.5, being summarized by a great alternation in CD spectrum, diminishing LD spectrum and extrusion of intercalated ethidium. At the low Zn^{2+} concentration range, the appearance of the CD spectrum in the DNA absorption region is in sharp contrast with that at pH 7.0 although the LD decreases a little and ethidium remains to intercalate, indicating that the secondary structures of DNA differ at pH 7.0 and 8.5. At pH 8.5, appearance of a positive band near 265 nm implies at least part of DNA is in the A-form. The difference between the two pHs is further discussed in the following section.

As the Zn^{2+} concentration increases, transition from B-form DNA (at low Zn^{2+} concentration form to be distinguished from ordinary B-form) to M-DNA occurs. The transition seems to occur between the two states, as is suggested by the existence of the isodichroic point in the CD spectra. The local secondary structure of M-DNA is conceivably in C-form which is different from the ordinary B form and also from that at the low Zn^{2+} concentrations. However, the disappearance of the LD magnitude indicates that M-DNA does not orient in the flow because the optical factor in the current experimental condition was not changed. The reasons causing a decrease in the ability to orient include changes in temperature and viscosity of the medium which were not changed in the experiment. Therefore, the only reasons remaining are the changes in the DNA contour length and the (local) denaturation of DNA. Since we did not find any evidence for denaturation of DNA, the decrease in the DNAs contour length is the most probable reason for the decrease in the LD magnitude. Considering that the secondary structure of DNA also remained as an overall right handed double helix, it is conceivable that DNA is aggregated and shortened in its M form in a high Zn^{2+} concentration. Although the metal ions are different, an average of five fold shortening in the contour length upon formation of M-DNA in the presence of either Ni^{2+} or Co^{2+} ions has been reported by atomic force microscopy [7]. The height of M-DNA is almost one order higher compared to that of B-DNA.

4.2. Conformation of DAPI in M-DNA

Three binding modes for DAPI that bound to DNA and synthetic adenine-thymine rich polynucleotides have been reported based on their characteristic induced CD spectrum [8,10]. At a low DAPI to DNA concentration ratio, induced CD spectrum of DNA or poly[d(A-T)$_2$] bound DAPI is characterized by a positive band with its maximum at 335 nm and a shoulder at 365 nm (Type I). As the [DAPI]/[DNA] ratio increases, the CD induced per DAPI molecule is redistributed to give a CD maximum at 365 nm with shoulder at 340 nm (Type II). An isosbestic point at 341 nm for poly[d(A-T)$_2$] and 351 nm for DNA exists, indicating the presence of two

spectroscopic species. At a high [DAPI]/[DNA] ratio, reduction of the CD band at 375 nm and a very small negative CD band at 425 nm was observed (Type III). From the thorough spectroscopic study using various oligonucleotides and polynucleotides, Type II CD spectrum was attributed to an allosteric binding such that when DAPI molecules bind contiguously to the AT sequence the conformation of the latter binding site changed [10]. The origin of Type III CD spectrum of the DNA-bound DAPI is less certain but it is believed to be the DAPI molecules that bound to the surface of the minor groove that is narrowed by the presence of Type I and II DAPI. Given this information, the mixing ratio dependent CD spectrum of the DAPI–DNA complex at pH 7.0 at high Zn^{2+} concentrations, which appears to be similar to that in the absence of Zn^{2+}, may be understood by the same binding conformation. Hence, it is conclusive that the binding of the Zn^{2+} to the phosphate groups of DNA does not affect the binding conformation of DAPI at pH 7.0. From the LD^r result, the presence of Zn^{2+} did not affect the angle between the transition moment of DAPI and the local DNA helix axis. Overall LD^r magnitude seems to be increased, which may be due to the change in the secondary structure of DNA although it is not certain.

The facts, that appearance of CD spectrum of DAPI bound to DNA at pH 8.5 and a high Zn^{2+} concentration resembles to that of type III, and that magnitude of the positive CD in the DAPI absorption region decreased as the [DAPI]/[DNA] ratio increased, suggest the environment of DAPI of these two condition resemble. This species is accessible to the I_2 quencher and hence, is exposed more to the solvent than Type I and II. Therefore, it is conceivable that DAPI cannot bind deep in M-DNA. In B-DNA case, the minor groove binding of DAPI which requires formation of hydrogen bonds with DNA bases in addition to the hydrophobic effect provided by the narrow groove. Hence it is suggestive that the hydrogen bonding sites are already occupied by Zn^{2+} ions. This analysis leads to the conclusion that Zn^{2+} bind at the minor groove side of DNA. The LD^r spectrum observed at pH 8.5 at the intermediate Zn^{2+} concentrations may be attributed to the B-DNA (again to be distinguished from ordinary B-DNA, some A-form character may be involved) although the angle of DAPI transition with respect to the local DNA helix axis is smaller than that in the absence of Zn^{2+} ions. In other words, the LD^r at intermediate Zn^{2+} concentrations represent the coexistence of B- and M-DNA.

5. Conclusion

DAPI binds at the surface of M-DNA at which the environment of DAPI resembles to that observed from type III binding mode. Zn^{2+} ions may locate at the site that corresponding to the minor groove of B-DNA thereby preventing Type I and II binding of DAPI in M-DNA.

Acknowledgements

This work was supported by the Korean Science and Engineering Foundation (Grant no. R01-2005-000-10490-0).

References

[1] S.D. Wettig, C.-Z. Li, Y.-T. Long, H.-B. Kraatz, J.S. Lee, M-DNA: a self-assembling molecular wire for nanoelectronics and biosensing, Anal. Sci. 19 (2003) 23–26.
[2] Y.-T. Long, C.-Z. Li, T.C. Sutherland, H.-B. Kraatz, J.S. Lee, Electrochemical detection of single-nucleotide mismatches: application of M-DNA, Anal. Chem. 76 (2004) 4059–4065.
[3] R.P. Janek, W.R. Fawcett, A. Ullman, Impedance spectroscopy of self-assembled monolayers on Au(III): sodium ferrocyanide charge transfer at modified electrodes, Langmuir 14 (1988) 3011–3018.
[4] P. Aich, S.L. Labiuk, L.W. Tari, L.J.T. Delbaere, W.J. Roesler, K.J. Falk, R.P. Steer, J.S. Lee, M-DNA: a complex between divalent metal ions and DNA which behaves as a molecular wire, J. Mol. Biol. 294 (1999) 477–485.
[5] A. Rakitin, P. Aich, C. Papadopoulos, Y. Kobzar, A.S. Vedeneev, J.S. Lee, J.M. Xu, Metallic conduction through engineered DNA: DNA nanoelectronic building blocks, Phys. Rev. Lett. 86 (2001) 3670–3673.
[6] J.S. Lee, L.J.P. Latimer, R.S. Reid, A cooperative conformational change in duplex DNA induced by Zn^{2+} and other divalent metal ions, Biochem. Cell. Biol. 71 (1993) 162–168.
[7] F. Moreno-Herrero, P. Herrero, F. Moreno, J. Colchero, C. Gómez-Navarro, J. Gómez-Herrero, A.M. Baró, Topographic characterization and electrostatic response of M-DNA studied by atomic force microscopy, Nanotechnology 14 (2003) 128–133.
[8] B. Nordén, S. Eriksson, S.K. Kim, M. Kubista, R. Lyng, B. Åkerman, in: B. Pullman, J. Jortner (Eds.), Molecular Bases of Specificity in Nucleic Acid–Drug Interactions, Kluwer Academic Publishers, Amsterdam, 1990, pp. 23–41.
[9] G.F. Loontiens, L.W. McLaughlin, S. Diekmann, R.M. Clegg, Binding of Hoechst 33258 and 4',6-diamidino-2-phenylindole to self-complementary decadeoxynucleotides with modified exocyclic base substituents, Biochemistry 30 (1991) 182–189.
[10] S. Eriksson, S.K. Kim, M. Kubista, B. Nordén, Binding of 4',6-diamidino-2-phenylindole (DAPI) to AT regions of DNA: evidence for an allosteric conformational change, Biochemistry 32 (1993) 2987–2998.
[11] H.-K. Kim, J.-M. Kim, S.K. Kim, B. Nordén, Interactions of intercalative and minor groove binding ligands with triplex poly(dA)·$[poly(dT)]_2$ and with duplex poly(dA)·poly(dT) and $poly[d(A-T)]_2$ studied by CD, LD, and normal absorption, Biochemistry 35 (1996) 1187–1194.
[12] T.A. Larsen, D.S. Goodsell, D. Cascio, K. Grzeskowiak, R.E. Dickerson, The structure of DAPI bound to DNA, J. Biomol. Struct. Dyn. 7 (1989) 477–491.
[13] S. Mohan, N. Yathindra, A study of the interaction of DAPI with DNA containing AT and non-AT sequences–molecular specificity of minor groove binding drugs, J. Biomol. Struct. Dyn. 9 (1994) 695–704.
[14] E. Trotta, E. D'Ambrosio, N. Del Grosso, G. Ravagnan, M. Cirilli, M. Paci, 1H NMR study of $[d(GCGATCGC)]_2$ and its interaction with minor groove binding 4′,6-diamidino-2-phenylindole, J. Biol. Chem. 268 (1993) 3944–3951.
[15] D. Vlieghe, J. Sponer, L. Van Meervelt, Crystal structure of d(GGCCAATTGG) complexed with DAPI reveals novel binding mode, Biochemistry 38 (1999) 16443–16451.
[16] R. Lyng, A. Rodger, B. Nordén, The CD of ligand–DNA systems. I. Poly(dG–dC) B-DNA, Biopolymers 31 (1991) 1709–1720.
[17] B. Nordén, M. Kubista, T. Kurucsev, Linear dichroism spectroscopy of nucleic acids, Q. Rev. Biophys. 25 (1992) 151–170.
[18] B. Nordén, T. Kurucsev, Analysing DNA complexes by circular and linear dichroism, J. Mol. Recognit. 7 (1994) 141–156.
[19] A. Rodger, B. Nordén, Circular Dichroism and Linear Dichroism, Oxford University Press, New York, 1997, pp. 33–34.
[20] Y. Matsuoka, B. Nordén, Linear dichroism studies of nucleic acids. II. Calculation of reduced dichroism curves of A- and B-form DNA, Biopolymer 21 (1981) 2433–2452.
[21] Y. Matsuoka, B. Nordén, Model for the irreversible dissociation kinetics of cooperatively bound protein–nucleic acid complexes, Biopolymer 22 (1982) 1713–1734.
[22] B. Nordén, S. Seth, Critical aspects of measurement of circular and linear dichroism: a device for absolute calibration, Appl. Spectrosc. 39 (1985) 647–655.

[23] S.K. Kim, S. Eriksson, M. Kubista, B. Nordén, Interaction of 4',6-diamidino-2-phenylindole (DAPI) with poly[d(G-C)$_2$] and poly[d(G-m^{5}C)$_2$]: evidence for major groove binding of a DNA probe, J. Am. Chem. Soc. 115 (1993) 3441–3447.
[24] S.K. Kim, S. Eriksson, B. Nordén, Z→B transition in poly[d(G-m^{5}C)$_2$] induced by interaction with 4′,6-diamidino-2-phenylindole, Biopolymers 33 (1993) 1677–1686.
[25] U. Sehlstedt, S.K. Kim, B. Nordén, Binding of 4′,6-diamidino-2-phenylindole to [poly(dI–dC)]$_2$ and [poly(dG–dC)]$_2$: the exocyclic amino group of guanine prevents minor groove binding, J. Am. Chem. Soc. 115 (1993) 12258–12263.
[26] J.R. Lakowicz, Principles of Fluorescence Spectroscopy, 2nd ed., Plenum Press, New York, 2001, pp. 237–247.
[27] J.R. Lakowicz, Principles of Fluorescence Spectroscopy, 2nd ed., Plenum Press, New York, 2001, pp. 129–130.
[28] A.G. Szabo, D.T. Krajcarski, P. Cavatorta, L. Masotti, M.L. Barcellona, Excited state pKa behavior of DAPI. A rationalization of the fluorescence enhancement of DAPI in DAPI–nucleic acid complexes, Photochem. Photobiol. 44 (1985) 143–150.
[29] P. Cavatorta, L. Masotti, A.G. Szabo, A time-resolved fluorescence study of 4′,6-diamidino-2-phenylindole dihydrochloride binding to polynucleotides, Biophys. Chemist. 22 (1985) 11–16.
[30] M.L. Barcellona, E. Gratton, Fluorescence lifetime distributions of DNA-4',6-diamidino-2-phenylindole complex, Biochim. Biophys. Acta 993 (1989) 174–178.
[31] M.L. Barcellona, G. Cardiel, E. Gratton, Time-resolved fluorescence of DAPI in solution and bound to polydeoxynucleotides, Biochem. Biophys. Res. Commun. 170 (1990) 270–280.
[32] B. Jin, H.M. Lee, Y.-A. Lee, J.H. Ko, C. Kim, S.K. Kim, Simultaneous binding of meso-tetrakis(N-methylpyridinium-4-yl)porphyrin and 4′,6-diamidino-2-phenylindole at the minor grooves of poly(dA)poly(dT) and poly[d(A-T)$_2$]: fluorescence resonance energy transfer between DNA bound drugs, J. Am. Chem. Soc. 127 (2005) 2417–2424.
[33] M. Kubista, B. Åkerman, B. Nordén, Characterization of interaction between DNA and 4′,6-diamidino-2-phenylindole by optical spectroscopy, Biochemistry 26 (1987) 4545–4552.
[34] T.E. Wagner, V. Vandegrift, D.S. Moore, in: B.W. O'Malley, J.G. Hardman (Eds.), Circular Dichroism Analysis of Nucleoprotein Complexes, Methods in Enzymology, vol. XL, Academic Press, New York, 1975, pp. 209–238.
[35] S. Arnott, E. Selsing, The conformation of C-DNA, J. Mol. Biol. 98 (1975) 265–269.